Trivedi et al., J Powder Metall Min 2015, 4:1
http://dx.doi.org/10.4172/2168-9806.1000132

Powder Metallurgy & Mining

Research Article Open Access

Effect of Biofield Treatment on Structural and Morphological Properties of Silicon Carbide

Trivedi MK[2], Nayak G[2], Tallapragada RM[2], Patil S[2], Latiyal O[1] and Jana S[1]*

[1]*Trivedi Science Research Laboratory Pvt. Ltd., Hall-A, Chinar Mega Mall, Chinar Fortune City, Hoshangabad Road, Bhopal-462026, Madhya Pradesh, India*
[2]*Trivedi Global Inc., 10624 S Eastern Avenue Suite A-969, Henderson, NV 89052, USA*

Abstract

Silicon carbide (SiC) is a well-known ceramic due to its excellent spectral absorbance and thermo-mechanical properties. The wide band gap, high melting point and thermal conductivity of SiC is used in high temperature applications. The present study was undertaken to investigate the effect of biofield treatment on physical, atomic, and structural characteristics of SiC powder. The control and biofield treated SiC powder was analysed using X-ray diffraction (XRD), particle size analyzer, surface area analyzer, and Fourier transform infrared (FT-IR) spectroscopy techniques with respect to control. The XRD pattern revealed that crystallite size was significantly increased by 40% in treated SiC as compared to control. The biofield treatment has induced changes in lattice parameter, density and molecular weight of atoms in the SiC powder. Particle size was increased upto 2.4% and the surface area was significantly reduced by 71.16% in treated SiC as compared to control. The FT-IR results indicated that the stretching vibrations frequency of silicon-carbon bond in treated SiC (925 cm^{-1}) was shifted towards lower frequency as compared to control (947 cm^{-1}). These findings suggest that biofield treatment has substantially altered the physical and structural properties of SiC powder.

Keywords: Biofield treatment; Silicon carbide; X-ray diffraction; FT-IR; Particle size; Surface area

Introduction

Ceramics have been used for many years in structural, abrasive and electronics devices; and mostly are metal oxides. However, nowadays new ceramics like nitrides, carbides also grab significant attention due to their unique characteristics, such as high melting point, hardness and excellent mechanical and electronic properties. The silicon carbide (SiC), naturally exists in about 250 crystalline forms [1]. Out of them, two most commonly recognized forms of SiC are: cubic (β-SiC) and hexagonal (α-SiC) (Figure 1). The α-SiC crystalline form exists : 2H-SiC, 4H-SiC, and 6H-SiC as per number of hexagonal layer present in a unit cell; for instance 6H-SiC have six layers [2,3]. In microelectronic devices, and high temperature applications, the energy band gap and electron mobility of SiC plays a crucial role, which are closely associated with its crystal structure, lattice strain, dislocations density and crystallinity [4]. The SiC powders can be synthesized via various processes such as Acheson process (solid state reaction between sand and coke at 2500°C), liquid phase reactions, carbothermal reduction method, physical vapour deposition, pyrolysis, and chemical vapor deposition [5,6]. Most of the above processes require a very high temperature (>1500°C) for better control over particle size, surface area and crystal structure of SiC. Recently, some other techniques such as high energy milling, mechanical alloying (or ball milling), reaction milling also have been employed to control the particle size, surface area and crystal structure parameters [7-9].

The biofield is a cumulative outcome of electric and magnetic field, exerted by the human body [10]. It is generates through some internal dynamic processes such as blood flow, lymph flow, brain and heart function in the human body. Recently, Mr. Trivedi's biofield has made significant breakthrough in various research areas such as material science [11-18], biotechnology [19,20], microbiology [21-23], and agriculture [24-26]. This biofield treatment had also changed the particle size, surface area and lattice parameters in various ceramic powders such as Vanadium Pentoxide (V_2O_5), zirconium oxide (ZrO_2), and silicon dioxide (SiO_2) [16,17].

Based on the knowledge of existing literatures and considering the industrial significance of SiC, in present work an effort has been made to study the impact of biofield treatment on physical and structural properties of SiC.

Experimental

Silicon carbide (SiC) powder was procured from Sigma Aldrich, USA. The SiC powder sample was equally distributed into two parts. One part was considered as control and another part was subjected to Mr. Trivedi's biofield treatment. The treated part was further divided into four groups T1, T2, T3 and T4 and accessed on different time period. The control and treated samples were characterized using

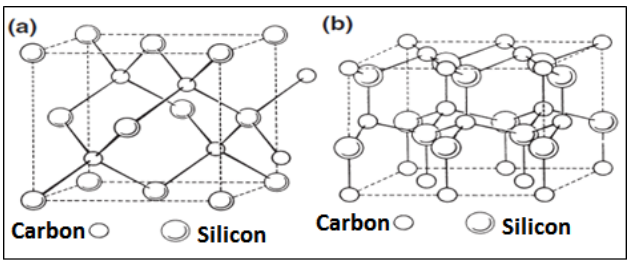

Figure 1: Crystal structures: (a) Zinc blend structure of 3C-SiC and (b) Wurtzite structure of 6H-SiC.

***Corresponding author:** Jana S, Trivedi Science Research Laboratory Pvt. Ltd., Hall-A, Chinar Mega Mall, Chinar Fortune City, Hoshangabad Road, Bhopal- 462026, Madhya Pradesh, India, Tel: +91-755-6660006; E-mail: publication@trivedisrl.com

Received June 18, 2015; **Accepted** June 25, 2015; **Published** July 07, 2015

Citation: Trivedi MK, Nayak G, Tallapragada RM, Patil S, Latiyal O, et al. (2015) Effect of Biofield Treatment on Structural and Morphological Properties of Silicon Carbide. J Powder Metall Min 4: 132. doi:10.4172/2168-9806.1000132

X-ray diffraction (XRD), particle size analyzer, surface area analyzer, and Fourier transform infrared (FTIR) spectroscopy.

X-ray diffraction study (XRD)

XRD analysis was carried out on X-ray diffractometer Phillips, Holland PW 1710 system, which had a copper anode with nickel filter. The radiation of wavelength used by this XRD system was 1.54056 Å. The data obtained from XRD were in the form of a chart of 2θ vs. intensity and a detailed Table 1 containing peak intensity counts, d value (Å), peak width (θ^0), relative intensity (%) etc. The PowderX software was used to calculate lattice parameter and unit cell volume. The crystallite size (G) was calculated by using formula:

$$G=k\lambda/(b\text{Cos}\theta),$$

Here, λ is the wavelength of radiation used and k is the equipment constant (=0.94). The molecular weight of a molecule was calculated as the sum of the atomic weight of all atoms. The atomic weight was calculated as the sum of the weight of all protons, neutrons and electrons present in the atom. The weight of the unit cell was computed as number of molecules present in a unit cell multiplied by the molecular weight of the molecules present. Whereas, the density was calculated as weight of the unit cell divided by volume of the unit cell. However, the percentage change in all parameters such as lattice parameter, unit cell volume, molecular weight, density, crystallite size was calculated using the following equation:

$$\text{Percent change in parameter} = [(a_t-a_c)/a_c] \times 100$$

Where, a_c and a_t are parameter value of control and treated powder samples respectively.

Particle size and surface area analysis

For particle size analysis, Laser particle size analyzer SYMPATEC HELOS-BF was used, which had a detection range of 0·1-875 µm. The particle size data was collected in the form of a chart of particle size vs. cumulative percentage. Surface area analyzer SMART SORB 90 BET was used for evaluation of surface area, which had a detection range of 0.1-1000 m^2/g.

Parameter	Control (day 1)	T1 (day 60)	T2 (day 90)	T3 (day 114)	T4 (day 130)
Lattice Parameter (Å)	3.0950	3.0927	3.0900	3.0926	3.0897
Percent change in Lattice Parameter		-0.08	-0.16	-0.08	-0.17
Unit cell Volume (10^{-22} cm^3)	1.259	1.257	1.255	1.257	1.254
Percent change in Unit cell Volume		-0.15	-0.33	-0.16	-0.34
Density (g/cc)	3.193	3.197	3.203	3.198	3.204
Percent change in Density		0.153	0.329	0.158	0.345
Molecular weight (g/mol)	40.34	40.28	40.21	40.28	40.20
Percent change in Mol. Weight		-0.15	-0.33	-0.16	-0.34
Crystallite Size (nm)	62.04	54.29	86.89	72.40	72.41
Percent change in Crystallite Size		-12.49	40.06	16.70	16.71

Table 1: Atomic and structural parameters of control and treated silicon carbide (SiC) calculated from XRD patterns.

Particle size	Control (day 1)	Treated T1 (day 12)	Treated T2 (day 85)	Treated T3 (day 92)	Treated T4 (day 100)
d_{50} (µm)	20.8	20.9	21.3	21.3	21.3
d_{99}(µm)	43.1	43.9	43.3	43.1	43.3

Table 2: The effect of biofield treatment on average particle size (d_{50}) and d_{99}.

FT-IR spectroscopy

FT-IR analysis was done on Shimadzu, Fourier Transform Infrared (FT-IR) Spectrometer with frequency range of 300-4000 cm^{-1}. The structural changes of control and treated samples T1, and T2 of SiC were evaluated on day 60 and day 100 respectively.

Results and Discussion

X-ray diffraction study

The lattice parameter of unit cell, volume of unit cell and densities of SiC were computed from XRD diffractogram using Powder X software, and results are reported in Table 2, Figures 2 and 3. It was found that lattice parameter of unit cell was reduced upto 0.17% in treated sample as compared to control (Figure 2). The decrease in lattice parameter in treated sample led to decrease in volume of unit cell up to 0.34% and consequently increased the density by 0.354% in treated SiC as compared to control (Figure 2). Furthermore, the percent change in lattice parameter and volume of unit cell in other treated SiC samples were found negative (Figure 4), which indicates that compressive stress may be applied on unit cell of SiC [27]. This compressive stress may be generated due to high energy milling through biofield treatment. Furthermore, the strain was existed even 130 days after biofield treatment (T4), which indicates that treated powder had compressive residual stress (Figure 2). Generally, residual stress occurs either through crystal structural change or plastic deformation. Since XRD result showed negative strain; and same crystal structure in control and treated SiC powder, which indicates that this compressive residual stress may be due to plastic deformation in treated SiC powder. Furthermore, the increased density should increase the molecular weight, but it was not observed in our experiment. Rather, the molecular weight of treated SiC sample was reduced by 0.354% as compared to control (Figure 2). It indicates that the number of protons/neutrons may alter after biofield treatment. It can be possible if weak reversible nuclear reaction takes place in treated SiC [28]. Moreover, the crystallite size (coherently scattering domains size) was reduced by 12.70% in treated T1 as compared to control (Figure 3). The presence of internal compressive lattice strain in SiC could be responsible to move the dislocations to the slip planes and built in stress concentration. This stress concentration might be increased to such extent and resulted into fracture the crystal at the sub boundaries and decreased crystallite size. Contrarily, the crystallite size was enlarged by 40.06%, 16.70%, and 16.71% in treated samples T2, T3 and T4 respectively (Figure 3). The increased crystallite size may be due to the crystallite growth through the movement of crystallite boundaries. Thus, it is hypothesized that high energy milling through biofield treatment may induce the movement of crystallite boundaries that results into large crystallite size. Kityk et al. reported that crystallite size and band gap are inversely proportional to each other [29]. Thus, it is speculated that the change in crystallite size through biofield treatment may led to alter the band gap in SiC powder.

Particle size and surface area analysis

The particle size result of control and treated samples are presented in Table 2 and Figure 4, which included the average particle sized$_{50}$ and d_{99} (size below which 99% of particles were present) and percent changes in treated SiC powder as compared to control. It was found that the average particle size d_{50}, increased up to 2.4% in treated SiC, whereas $d_{99,}$ increased by 1.9% as compared to control (Figure 4).

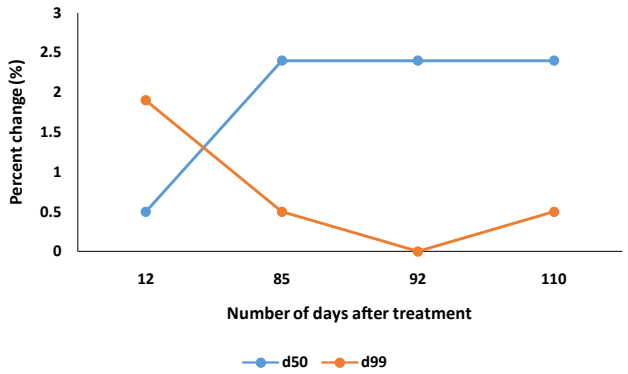

Figure 2: Percentage change in particle size d_{50} and d_{99} in biofield treated SiC as compared to control.

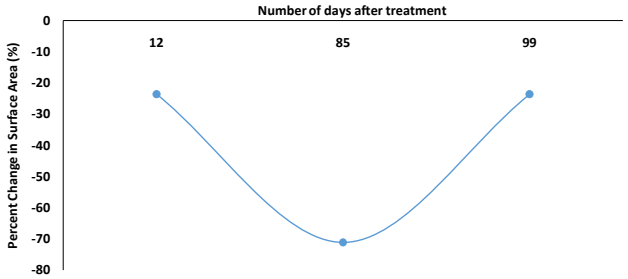

Figure 3: Percent change in surface area in biofield treated SiC as compared to control.

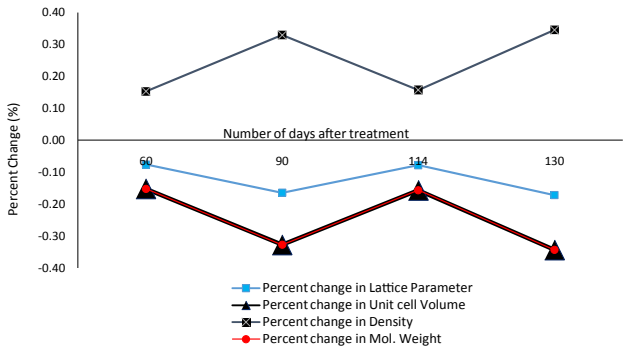

Figure 4: Percent change in XRD parameters of treated SiC sample as compared with control.

The graph showed that the percent change in d_{50}, increases and d_{99}, decreases with increase in number of days after treatment. It indicates that, the coarser particles may be fractured and transformed into finer particles after biofield treatment. Furthermore, the specific surface area was significantly decreased by 23.6%, 71.16% and 23.60% on day 12, day 85 and day 99, respectively as compared to control (Figure 5). This is possible when sharp corners with irregular shape like hills and valleys on the particle surfaces become rounded. Additionally, it is also possible that the smaller particles may come together and welded through surface diffusion [18].

FT-IR spectroscopy

IR spectrum of control and treated samples are illustrated in Figures

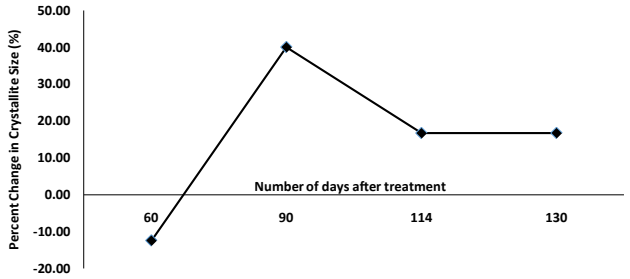

Figure 5: Percent change in crystallite size of treated SiC sample as compared with control.

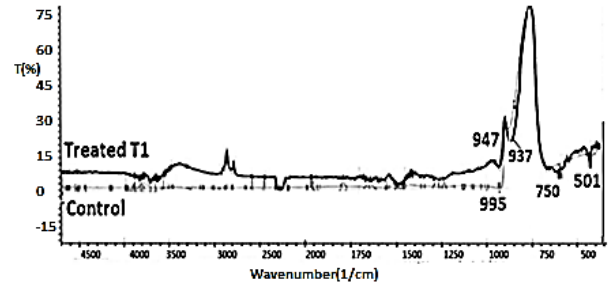

Figure 6: IR spectra of control and treated SiC powder sample T1.

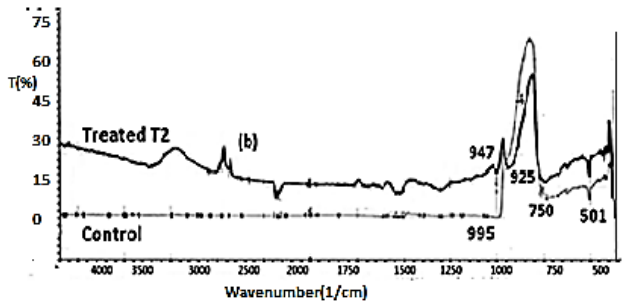

Figure 7: IR spectra of control and SiC powder treated sample T2.

6 and 7, respectively. The absorption peaks observed around 750 cm^{-1} and 937 cm^{-1} in treated and control samples, respectively, which were attributed to Si—C bond stretching vibrations [30]. Moreover, it was observed that absorption peaks at 947 cm^{-1} (control) was slightly shifted to lower wavenumber at 937 cm^{-1} (T1) and 925 cm^{-1} (T2) after treatment, which might be due to reduced bond strength and changed inter-atomic interactions through biofield treatment.

Conclusion

In summary, the biofield treatment has altered the particle size with the increment of 2.4% and significantly reduced the specific surface area by 71.16% in SiC powders. This could be due to change in particle shape and re-welding process caused by high energy milling through biofield treatment. Furthermore, the crystallite size in treated SiC powder was significantly changed as compared to control. Hence, the biofield treatment may affect the energy band gap of SiC. The shifting of IR peaks towards lower frequency revealed that silicon–carbon bond

stretching might alter through biofield treatment. This indicates that biofield might be acting at atomic level in SiC powder to cause these changes. Altogether, the study results suggest that biofield treated SiC powder might be useful for high temperature electronic device applications.

Acknowledgement

We thank Dr. Cheng Dong of NLSC, Institute of Physics, and Chinese academy of Sciences for supporting in using PowderX software for analysing X-ray Diffraction results.

References

1. Abderrazak H, Hmida ES (2011) Silicon carbide: Synthesis and properties. InTechpress.
2. Cheung R (2006) Silicon carbide micro electromechanical systems for harsh environments. Imperial College Press UK.
3. Li XB, Shi EW, Chen ZZ, Xiao B (2007) Polytype formation in silicon carbide single crystals. Diamond Relat Mater 16: 654-657.
4. Gyu J, Jin K, Jeong H, Kim Y, Makarov Y, et al. (2014) Evaluation of the change in properties caused by axial and radial temperature gradients in silicon carbide crystal growth using the physical vapor transport method. Acta Mater 77: 54-59.
5. Grosse P, Basset G, Calvat C, Couchaud M, Faure C, et al. (1999) Influence of reactor cleanness and process conditions on the growth by PVT and the purity of 4H and 6H SiC crystals. AdvFunct Solid State Mater 62: 58-62.
6. Snyder DW, Heydemann VD, Everson WJ, Barrett DL (2000) Large diameter PVT growth of bulk 6H SiC crystals. Mater Sci Forum 338-342: 9-12.
7. Chaira D, Mishra BK, Sangal S (2006) Synthesis of Silicon Carbide by Reaction Milling in a Dual-drive Planetary Mill. Society for Mining, Metallurgy and Exploration. Functional Fillers 253-265.
8. Mattieazzi P, Miani F (1993) Designing a high energy ball-mill for synthesis of nanophase materials in large quantities. Mater Sci Eng 168: 149-152.
9. Benjamin JS (1970) Dispersion strengthened superalloys by mechanical alloying. Metall Trans 1: 2943-2951.
10. Rubik B (2002) Thebiofield hypothesis: its biophysical basis and role in medicine. J Altern Complement Med 8: 703-717.
11. Trivedi MK, Tallapragada RM (2008) A transcendental to changing metal powder characteristics. Met Powder Rep 63: 22-28.
12. Trivedi MK, Tallapragada RM (2009) Effect of super consciousness external energy on atomic, crystalline and powder characteristics of carbon allotrope powders. Mater Res Innov 13: 473-480.
13. Dhabade VV, Tallapragada RM, Trivedi MK (2009) Effect of external energy on atomic, crystalline and powder characteristics of antimony and bismuth powders. Bull Mater Sci 32: 471-479.
14. Trivedi MK, Patil S, Tallapragada RM (2012) Thought intervention through biofield changing metal powder characteristics experiments on powder characteristics at a PM plant. Proceeding of the 2nd International Conference on Future Control and Automation 2: 247-252.
15. Trivedi MK, Patil S, Tallapragada RM (2013) Effect of biofield treatment on the physical and thermal characteristics of silicon, tin and lead powders. J Mater Sci Eng 2: 125-132.
16. Trivedi MK, Patil S, Tallapragada RM (2013) Effect of biofield treatment on the physical and thermal characteristics of vanadium pentoxide powder. J Mater Sci Eng 11:1-20.
17. Trivedi MK, Patil S, Tallapragada RM (2014) Atomic, crystalline and powder characteristics of treated zirconia and silica powders. J Mater Sci Eng 3: 144-152.
18. Trivedi MK, Patil S, Tallapragada RM (2015) Effect of biofield treatment on the physical and thermal characteristics of aluminium powders. IndEng Manage 4: 151-160.
19. Patil S, Nayak GB, Barve SS, Tembe RP, Khan RR (2012) Impact of biofield treatment on growth and anatomical characteristics of Pogostemoncablin (Benth). Biotechnology 11: 154-162.
20. Altekar N, Nayak G (2015) Effect of biofield treatment on plant growth and adaptation. J Environ Health Sci 1: 1-9.
21. Trivedi MK, Patil S, Bhardwaj Y (2008) Impact of an external energy on *Staphylococcus epidermis* [ATCC-13518] in relation to antibiotic susceptibility and biochemical reactions-An experimental study. J Accord Integr Med 4: 230-235.
22. Trivedi MK, Patil S (2008) Impact of an external energy on *Yersinia enterocolitica* [ATCC-23715] in relation to antibiotic susceptibility and biochemical reactions: An experimental study. Internet J Alternat Med 6: 13.
23. Trivedi MK, Patil S, Bhardwaj Y (2009) Impact of an external energy on *Enterococcus faecalis* [ATCC – 51299] in relation to antibiotic susceptibility and biochemical reactions - An experimental study. J Accord Integr Med 5: 119-130.
24. Shinde V, Sances F, Patil S, Spence A (2012) Impact of biofield treatment on growth and yield of lettuce and tomato. Aust J Basic Appl Sci 6: 100-105.
25. Lenssen AW (2013) Biofield and fungicide seed treatment influences on soybean productivity, seed quality and weed community. Agric J 8: 138-143.
26. Sances F, Flora E, Patil S, Spence A, Shinde V (2013) Impact of biofield treatment on ginseng and organic blueberry yield. AGRIVITA J AgricSci 35: 132-141.
27. Gao F, Feng W, Wei G, Zheng J, Wang M (2012) Triangular prism-shaped p-type 6H-SiC nanowires. Cryst Eng Comm 14: 488-491.
28. Narlikar JV (1993) Introduction to cosmology, Jones and Bartlett Inc, Cambridge University Press .
29. Kityk IV, Kassiba A, Plucinski K, Berdowski J (2000) Band structure of large-sized SiC nanocomposites. Phys LettA 265: 403-410.
30. Ng SS, Hassan Z, Hassan HA (2007) Polarized infrared reflectance study of wurtziteGaN thin film: The effects of angle of incidence on the optical phonon modes. J Vac Sci Technol 25: 1557-1557.

Citation: Trivedi MK, Nayak G, Tallapragada RM, Patil S, Latiyal O, et al. (2015) Effect of Biofield Treatment on Structural and Morphological Properties of Silicon Carbide. J Powder Metall Min 4: 132. doi:10.4172/2168-9806.1000132